Impact Analysis of an Innovative Shock Energy Absorber and Its Applications in Improving Railroad Safety

Xudong Xin, Basant K Parida, Abdullatif K Zaouk, Norm Dana
QinetiQ North America, Technology Solution Group, 350 2nd Avenue, Waltham, MA 02451
and
Swamidas K Punwani
Office of Research and Development, Federal Railroad Administration, Washington, DC 20590

Abstract

There are over a hundred train collisions occurring in the United States each year. Engineers in QinetiQ North America (QNA) have applied LS-DYNA in locomotive crashworthiness simulations for years to help designing new railroad risk reduction techniques. This paper first describes the impact analysis technique used in QNA's recent development of an environment friendly ultra-high capacity shock energy absorber (SEA). The device utilizes the pressure-dependent reversible phase transition characteristics of Ultra High Molecular Weight Poly-ethylene (UHMW-PE) material. SPH method was used to model the energy absorbing process of the UHMW-PE material due to impact and penetration of a plunger. Finite element model was calibrated by the drop test of a prototype SEA. The test also confirmed the device's ultra-high energy absorption and damping capabilities. Results from FEA analysis enabled the scalability of the SEA for a range of practical applications.

Using detail SD70MAC locomotive model and open-top hopper car model developed by QNA, some train collision events have been analyzed. Among them, one simulated case recreated the collision scenario in which one freight train consisting of a SD70MAC locomotive hauling three loaded hopper cars traveled at 32.1 mph and collided on a stationary fully loaded 35-hopper car consist. Simulation result from the finite element model without applying SEA was validated with a full-scale locomotive crashworthiness test conducted by TTCI. Further, the LS-DYNA analysis results with the model having SEA units installed show the locomotive overriding the hopper car can be successfully prevented at same impact speed. There are many potential applications of the UHMW-PE based SEA units for safety enhancement such as using these units to improve rail tank car crashworthiness as well as the passenger train safety.

Keywords: finite element analysis, impact analysis, shock energy absorber, drop test, locomotive collision, crashworthiness, railroad safety, SPH, UHMW-PE

Introduction

Over the years, Federal Railroad Administration (FRA) has continued to support research programs and various efforts to benefit the railroad safety in the United States. This work is part of one program sponsored by FRA to improve locomotive crashworthiness and reduce the railroad collision severity by developing crash energy management (CEM) system to minimize the possibility of locomotive override during an in-line collision. New crashworthiness regulations, standards and recommended practices have been developed or updated in both U.S. and Europe by FRA, Association of American Railroads (AAR), American Public Transportation Association (APTA), and European Committee for Standardization (ECS) in recent years [1-6]. Based on the related locomotive design and performance standards, engineers in QNA have recently designed a new type of SEA which uses the special damping characteristics of UHMW-PE. New CEM systems for potential railroad applications can be developed using these innovative shock energy absorbers.

In this paper the authors discuss the finite element analysis techniques used in analyzing the prototype of UHMW-PE based SEA unit and also show the advantages of applying the SEA units in improving railroad safety through dynamic finite element simulations. Examples considered include SD70MAC locomotive impacting on open-top hopper car consist and tank car collisions.

Impact Analysis of QNA Shock Energy Absorber

To prevent locomotive override, a SEA unit must possess enough energy absorption capacity. It is impossible to fit a conventional oleo-pneumatic type of SEA at such capacity level within the limited under-frame space available in the locomotive crash zone. To overcome that limitation, the authors developed an innovative compact shock energy absorber for potential applications in freight locomotive crash energy management system. It uses a cost-effective UHMW-PE material as the damping material. The UHMW-PE body is confined in a steel cylinder and a steel plunger with a conical-shape front facing the top center of UHMW-PE. High speed impact will cause plunger to penetrate into the UHMW-PE material and kinetic energy will be absorbed through plastic deformation and phase transition of UHMW-PE.

UHMW-PE Material

UHMW-PE is a semi-crystalline polymer. Previous tests conducted at QNA have shown this material can undergo a reversible phase transition between solid state and viscous fluid state when the compressive stress exceeding or dropping below a critical value. Dynamic tests revealed that the critical stress value for phase transition depends on both the loading rate and the confinement. In other words, the peak value of dynamic force developed during high speed impact depended on the impact velocity as well as on the ratio of the cross-sectional area of UHMW-PE material to that of the plunger (Figure 1).

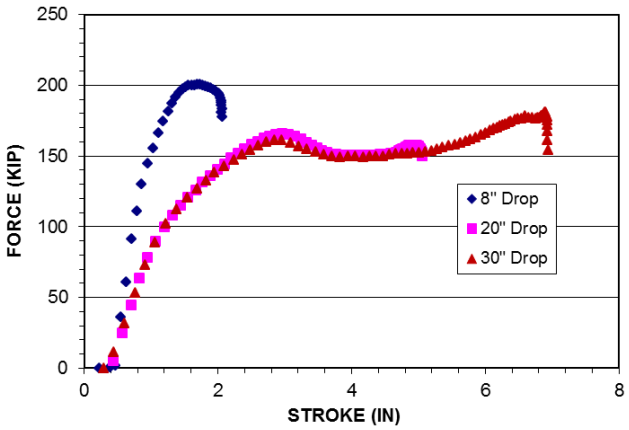

Figure 1 Effects of impact speed on UHMW-PE loading path with a 27,000 lbf drop weight.

When the steel plunger penetrates into the UHMW-PE cylinder core during an impact event, UHMW-PE material in a small zone in front of the plunger will be compressed and transformed into viscous fluid state as the critical compressive stress is reached. The UHMW-PE material in viscous fluid state around the plunger front will flow away from this high pressure domain to the low pressure domain. To suitably analyze this kind of large deformation process without tackling mesh tangling issue, the Smoothed Particle Hydrodynamics (SPH) method was adopted to simulate the penetration process. LS-DYNA material type *MAT_ELASTIC_PLASTIC_

HYDRO [7] was used for UHMW-PE material with the plastic strain at failure set to 50% to represent the critical point at which the material enters a plastic flow state through phase transition. Material parameters of UHMW-PE for a 30 in drop test were set as follows: shear modules G = 3,5741psi, density ρ = 0.0336 lb/in^3, yield stress σ_y = 4,800 psi and plastic hardening modulus E_h = 6,400 psi. An equation of state (EOS) of the type *EOS_LINEAR_ POLYNOMIAL was employed to calculate the pressure change of UHMW-PE material. This can ensure that UHMW-PE particles still exert resistant force on plunger by pressure even in failure state. Material properties for the cylinder, plunger, outer sleeve, manifold and bush bearing were determined based on the specific prototype design information. Because of the extremely high strength requirement, the seamless cylinder and plunger are made of high strength low alloy (HSLA) steel. The outer sleeve and manifold next to the bronze bush bearing was made of cold drawn steel.

Contact interfaces of the type *CONTACT_AUTOMATIC_SURFACE_TO_SURFACE were defined between plunger, bush bearing, sleeve, manifold and cylinder. Contact between SPH particles and all other adjacent parts provided not only the resistance force to the motion of plunger, but also the confining pressure to UHMW-PE. Any missing master segments can lead to a leakage problem to the confining boundary condition. This interface was defined in the type of *CONTACT_ AUTOMATIC_NODES_TO_SURFACE. Based on data available in the published specification sheet from the manufacturers of UHMW-PE material, the static and dynamic coefficient of friction between UHMW-PE and steel parts was taken as 0.15 and 0.12, respectively.

Figure 2(a) shows the prototype of SEA to be tested with a 3 inch diameter plunger. The corresponding full scale finite element model (see Figure 2(b)) consists of 486,100 nodes, 47,600 solid/thick shell elements, 421,200 SPH particles and 16 parts in LS-DYNA. The flange-end of the steel cylinder was fixed in space in axial direction. The initial speed of the 27,000lbf impacting mass was assigned to 152.28 in/sec, corresponding to a 30 inch free fall of the hammer in test. Figure 2(c) shows the calculated pressure contours on a center-cut profile after 50ms following the impact. Figure 2(d) shows the von-Mises stress contours at the same time.

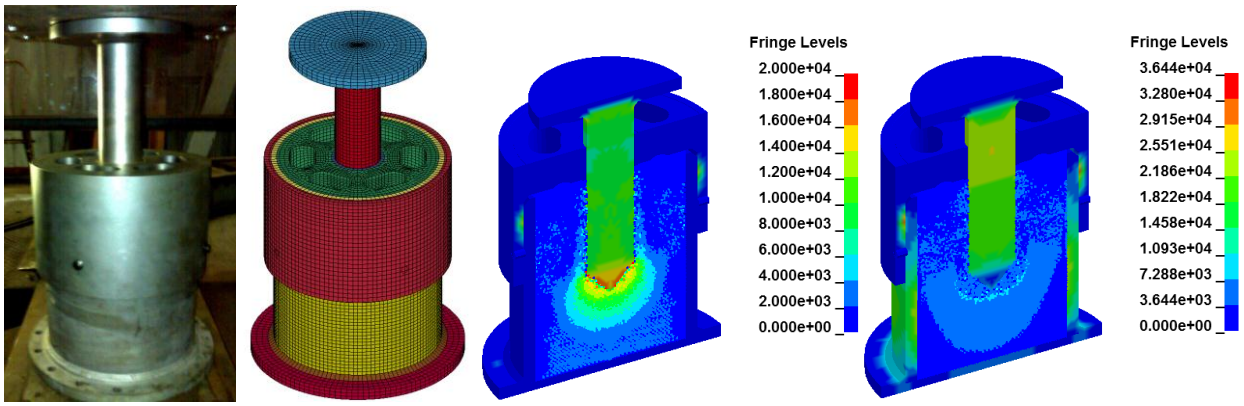

(a) Pre-test photo (b) FE model (c) Pressure contour (d) von-Mises stress contour

Figure 2 (a) Pre-test photo; (b) a full SEA model; (c) the pressure contour at t = 50 ms; (d) the von-Mises stress contour at t = 50ms.

The zone featured with high pressure (Figure 2(c)) and low von-Mises stress (Figure 2(d)) around the plunger front reflects there is a viscous fluid zone surrounding the plunger front. A sequence of effective plastic strain fringes is shown in Figures 3(a) to 3(d), which clearly reveals the time variation of the domain of influence from plunger penetration.

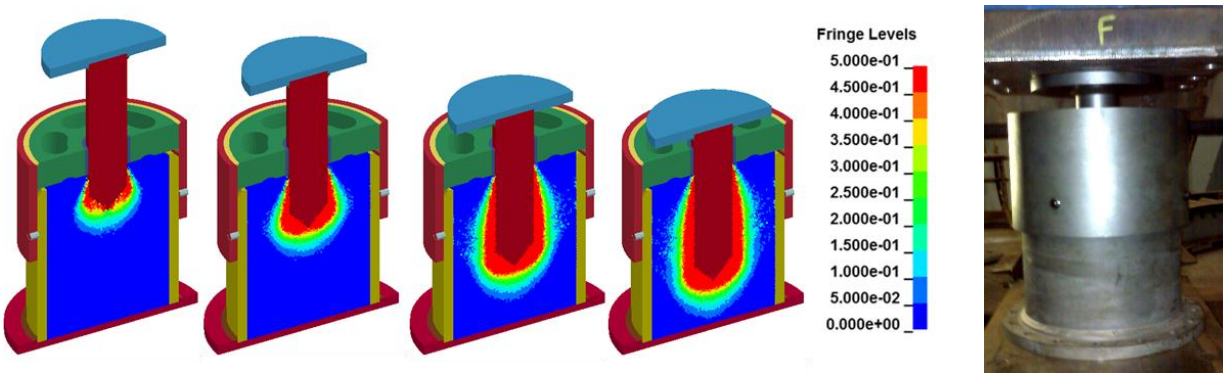

(a) t = 10 ms (b) t = 20 ms (c) t = 50 ms (d) t = 80 ms (e) Post-test photo

Figure 3 Time sequence of effective plastic strain contours in UHMW-PE and post-test photo.

When a SPH particle reaches the failure effective plastic strain (ε_p= 0.5), it can be considered that its phase changes into viscous fluid state. Therefore, the volume occupied by these SPH particles represents the viscous fluid domain. As shown in Figures 4(a) to 4(e), a single connecting viscous fluid zone developed until t = 16 ms after impact. At that time, the plunger already traveled about 2.3 inches inside UHMW-PE (Figure 5). The force value corresponding to 2.3 inch displacement on the force vs. displacement curve (Figure 6) represents the critical force for UHMW-PE phase change. It has been observed that viscous UHMW-PE material oozing out of the core along the plunger shaft surface soon after impact tests or when the UHMW-PE core was cut. The viscous UHMW-PE material solidified as soon as pressure was released.

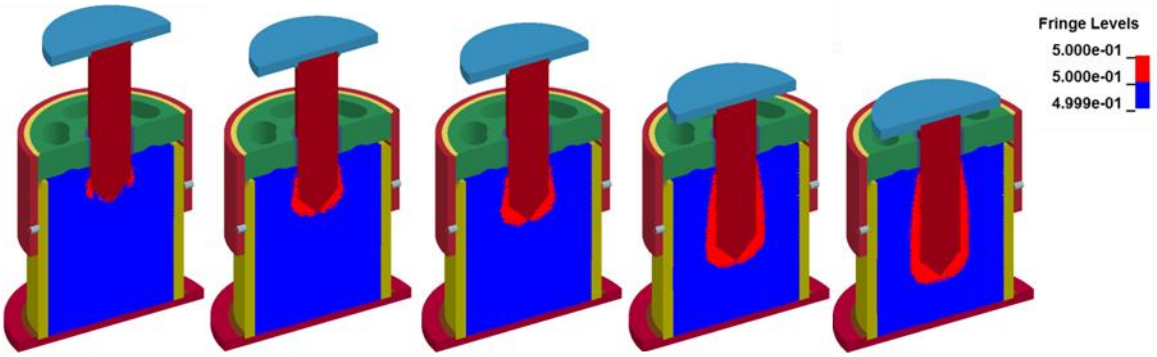

(a) t = 10ms (b) t = 16ms (c) t = 20ms (d) t = 50ms (e) t = 80ms

Figure 4 Predicted size of fluid zone (red) developing with time

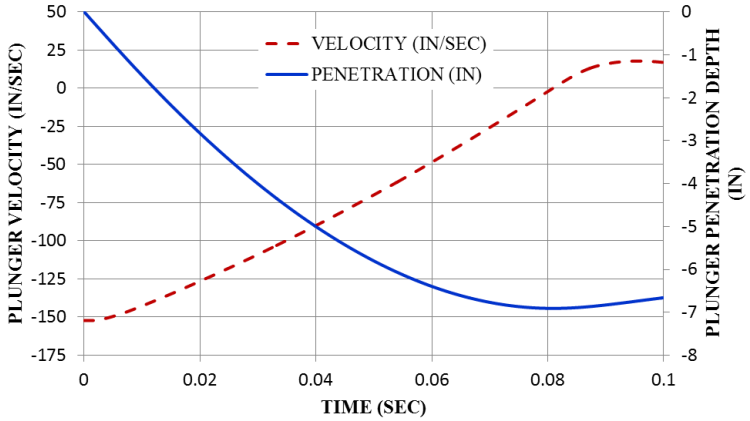

Figure 5 Time history plots of plunger velocity and penetration depth.

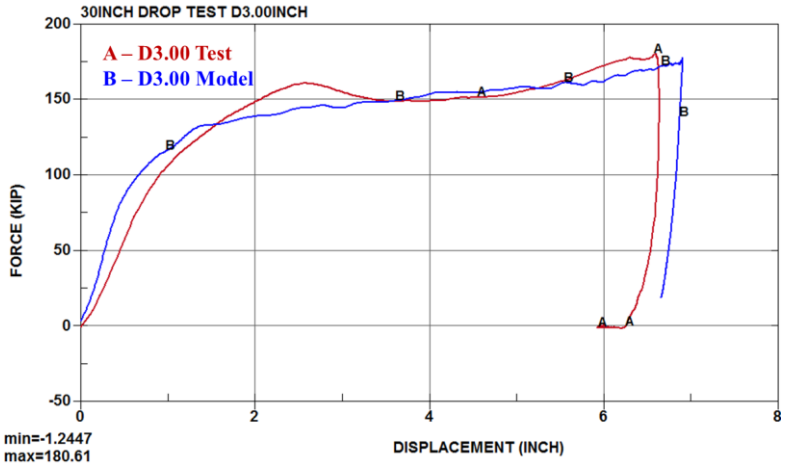

Figure 6 Dynamic force versus plunger displacement plots from test and FEA.

The prototype SEA unit (Figure 2(a)) with 80,000 ft-lbf energy absorbing capacity was designed and fabricated for the drop hammer test to be conducted at ASF-Keystone facility in Pennsylvania. The test was intended to validate the geometric size effects of SEA for future railroad crashworthiness applications. Test result showed crash energy from the 30 inch drop of a 27,000 lbf hammer was fully absorbed by the SEA unit (Figure 3(e)). The penetration depth of the plunger and the peak compression force were measured which match well with the prediction from LS-DYNA calculations. Plots of dynamic axial force in plunger versus plunger penetration depth from both the FEA result and the drop test data are shown in Figure 6. The area under the force versus displacement graph represents the amount of kinetic energy and gravity work absorbed by the UHMW-PE material in reducing the plunger velocity from 152.28 in/sec to zero within a total plunger penetration depth of 6.90 inch. The area under this curve is found to be 971,070 in-lbf. Comparing this value to 987,390 in-lbf, which is the total energy released by gravity during a total 36.57 inch drop for a 27,000 lbf weight in test, the FEA prediction for energy absorbed is only 1.65% less than the actual value (Table 1).

Table 1 Comparison between Test Data and FEA Results

Data	Penetration Depth (in)	Peak Axial Force (kip)	Energy Absorbed (in-lbf)
Test	6.57	180.61	987,390*
FEA	6.90	178.14	971,070
Error	+0.50%	-1.37%	-1.65%

**Calculated from a 36.57in drop of 27,000lbf weight.*

SEA Applications in Railroad Crashworthiness Research

The uses of crash energy management (CEM) system can greatly reduce the collision force between impacting vehicles, it can in turn lower the structural damage and increase crew survival space. Based on federal locomotive design and performance standards, engineers in QNA have designed a new CEM system by using above innovative shock energy absorbers.

Figures 7(a) and (b) show the bottom views of the CAD drawing and the finite element model of the designed CEM system that has been assembled on the under-frame of a SD70MAC locomotive model, respectively. The system made of seven SEA units with a central one installed on the sill plate behind the draft gear pocket and other six units installed between the added plates and the pilot plates. The central unit has the maximum capacity since it is on the main loading path during a collision. To reduce the computational cost, these SEA units were modeled as non-linear springs. Figure 8 shows the loading/unloading characteristics for all SEA springs used in this simulation.

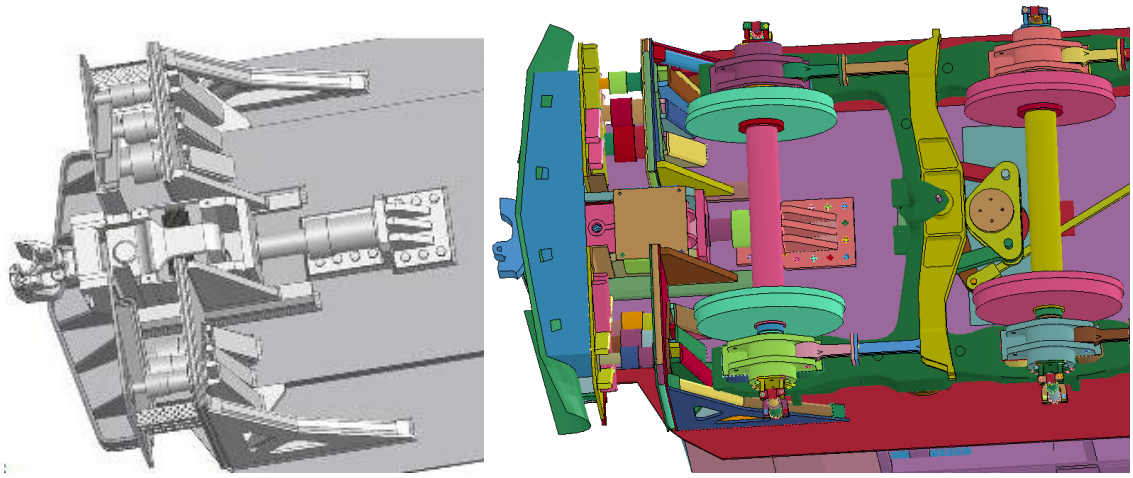

(a) (b)

Figure 7 Bottom views of CEM System: (a) CAD drawing showing SEA units integrated to a SD70 locomotive; (b) corresponding finite element model of SD70 with CEM added

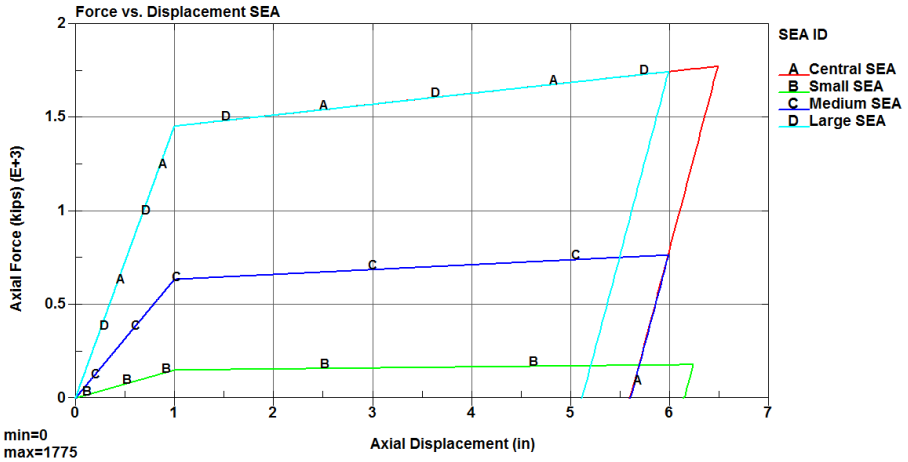

Figure 8 Loading/unloading paths of springs representing SEAs with different capacities

Finite element models for a standard EMD SD70MAC locomotive and an open-top hopper car model have been developed in QNA for crashworthiness simulation (Figures 9 and 10). The SD70MAC model uses a total of 386,711 nodes, 316,508 elements, 368 parts and it weighs 415,000 lbf. The open-top hopper car model was developed using the available hopper car data of Union Pacific Railroad (UP). The model has 50,079 nodes, 42,029 element, 55 parts and it weighs 60,000 lbf. The total weight will be 260,000 lbf if it is fully loaded. The ends of both the locomotive and the open-top hopper car models use finer mesh for better contact performance.

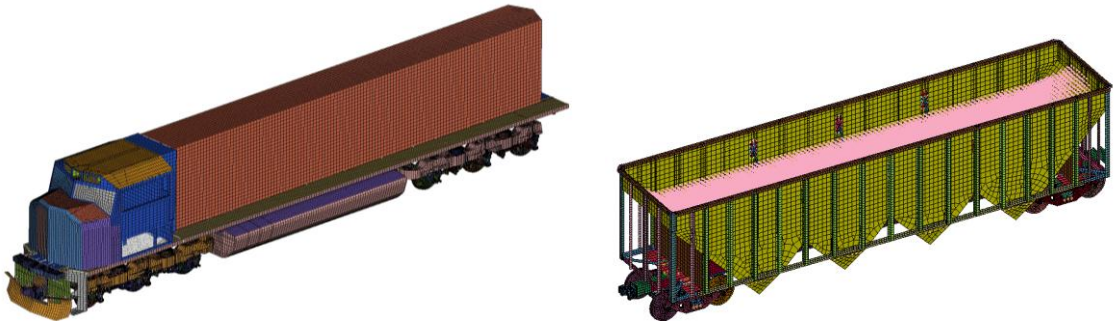

(a) (b)

Figure 9 FEA models of (a) a standard SD70MAC locomotive and (b) an open-top hopper car model loaded with coal

Simulation of Collision between a Locomotive and a Hopper Car Consist

Much effort of previous researches on locomotive collision modeling can be taken as references in current studies [e.g. 8-9]. To see the safety improvement of using CEM on SD70MAC, and ensure the vehicle models can correctly represent the structural integration of the SD70MAC locomotive and open-top hopper car model, a calculation was performed to simulate an actual impact test conducted previously by Transportation Technology Center, Inc. (TTCI), Pueblo, Colorado. The available test results were used to validate the built locomotive and open-top hopper car models. In the simulated collision event, a freight train consisting of one SD70MAC locomotive hauling three loaded open-top hopper cars traveled at 32.1 mph and collided on a stationary fully loaded 35-hopper car consist. The moving freight consist including locomotive unit weighed totally 1,185,900 lbf and was about 206 ft in length. The stationary freight consist weighed 9,100,000 lbf. The loaded coal mass inside the first hopper car was modeled by SPH particles. SPH method is a good choice for modeling continuous changes in contact force and mass distribution during impact. It is known that impact analysis often involves mesh tangling and solid element erosion due to large deformation. Eroding solid element at failure can cause mass loss as well as contact force reduction. However, using SPH method can avoid these disadvantages in this calculation. It successively simulated coal mass distribution changing as the locomotive front intruded inside the hopper car. Coal mass was conserved and its resistance to locomotive front intrusion has been maintained.

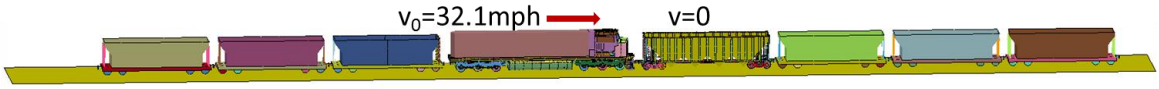

Figure 10 Impact simulation scenario is similar to the test done by TTCI.

In the simulation, only the hopper car directly faced the locomotive front used the fine hopper car model. To save CPU time, all other hopper cars were modeled using a coarse mesh hoper car model with only 2016 elements and 42 parts per car. The simulation used only 4 hopper cars representing the stationary fully loaded 35-hopper car consist. The first three hopper cars have the same fully loaded weight – 260,000 lbf. The fourth hopper car model stands for the rest 32 fully loaded cars and its model weight as well as its coupler and draft gear stiffness are equivalent to that of 32 loaded hopper cars. Besides contact interfaces specified for structural integration purpose in each car model, a contact interface of the type *CONTACT_ AUTOMATIC_SINGLE_SURFACE was defined for the parts possibly involving in contacting during impact process. The interaction between coal (SPH particles) and the confining parts of

hopper car and impacting parts of locomotive front was described through a contact surface of the type *CONTACT_AUTOMATIC_NODE_TO_SURFACE. The locomotive train consist was prescribed with initial translational velocity of 32.1 mph and the angular velocity of the wheels about the wheel rotational axes were preset at 20.1 rad/sec.

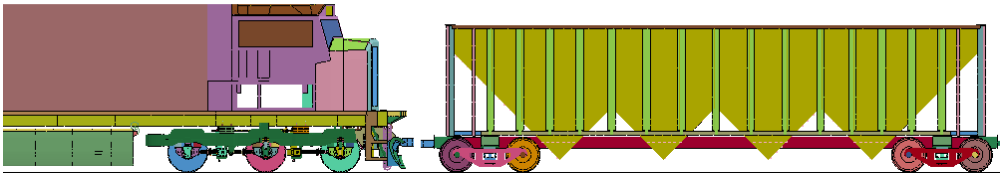

(a) Model at t = 0

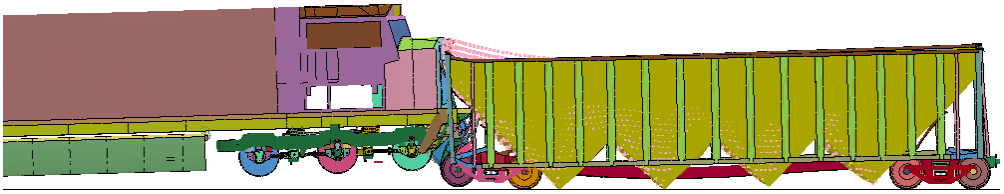

(b) t = 300 ms

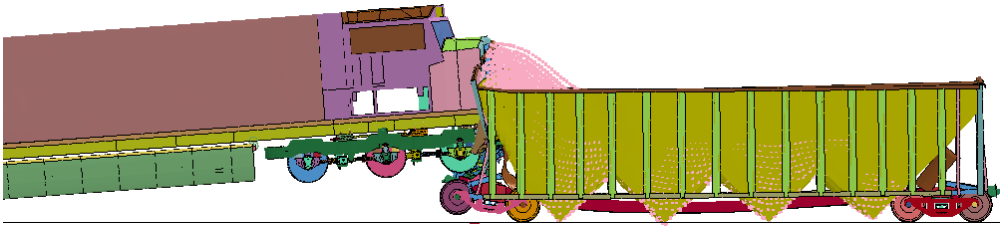

(c) t = 500 ms

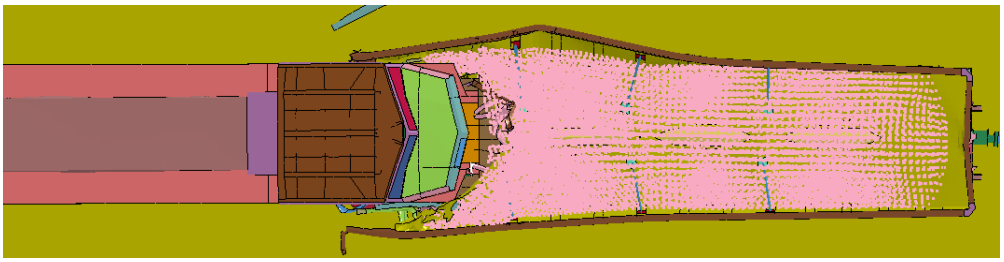

(d) t = 800ms

Figure 11 Collision simulation of SD70 without CEM: (a) - (c) side view t = 0 to 500 ms; (d) top view at t = 800ms after collision

Figure 11 shows simulation results for the standard SD70MAC locomotive impacting on the stationary hopper car consist at 32.1 mph. Figure 11(a) shows the initial collision configuration. At t = 300 ms (Figure 11(b)), the locomotive pilot plates deformed to create a kind of ramps that facilitate locomotive front-end override over the hopper car trucks. Figure 11(c) shows the locomotive front end overriding the truck of hopper car at t = 500 ms. It can be seen that the front-end of locomotive had completely entered the hopper car truck from the top view at t = 800 ms.

Correspondingly, Figure 12 shows frames captured from the TTCI crashworthiness test video at similar post-crash moments i.e. at t = 0, 300 ms and 500 ms, respectively. Comparing the deformation and progression of locomotive override between simulation and TTCI test, it is clear that the simulation has successively re-created the overall locomotive overriding dynamics.

(a) t = 0

(b) t = 300 ms

(c) t = 500 ms

Figure 12 Images from the TTCI test video: (a) at t = 0 - just before collision; (b) at t = 300 ms; (c) at t = 500 ms.

Simulation of Collision between a Locomotive with CEM and a Hopper Car Consist

To predict the performance of CEM using UHMW-PE based SEA units, the SD70MAC locomotive model with CEM system was used in this simulation. As shown in Figure 7, the model added or modified the stiffened load transfer structure, the separable pilot plate and draft gear pocket, and seven SEA units within the locomotive fore-body structure. The whole CEM system added 169,372 nodes and 90,926 elements to the original SD70MAC model (Figure 13). For the simulation, the configuration of the stationary hopper car consist was unchanged. The initial traveling speed of the locomotive consist was still assigned at 32.1 mph which allows direct comparison of CEM system performance.

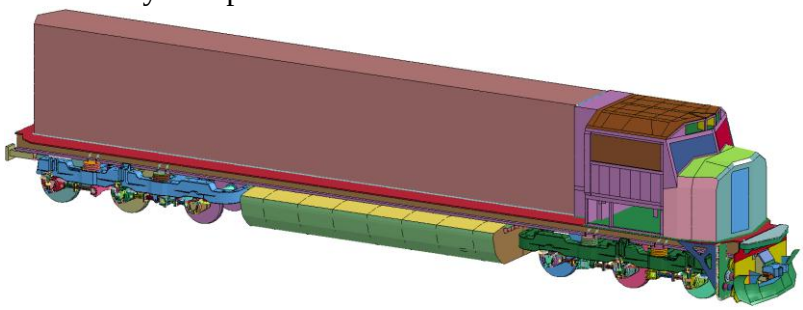

Figure 13 FEA model of a standard SD70MAC locomotive with CEM

Considering results in Figures 11 and 12, a comparable sequence of collision simulation for the locomotive with CEM system is shown in Figure 14. Simulation results show the energy dissipation and deformation control has maintained inline motion, creating large deformation in the first hopper car. The broken pilot plates do not form the ramp-like structure ahead of the

locomotive's front truck. This appears to prevent the locomotive fore-body from riding onto the hopper car. From Figure 14(b), it is observed that the locomotive front wheels have lifted about 4 inches from the rails, but the front wheels have dropped back onto the rails at t = 450 ms as shown in Figure 14(c) and Figure 16(b). The locomotive nose has severely crashed the hopper car structure and spilled the coal particles out of the hopper car.

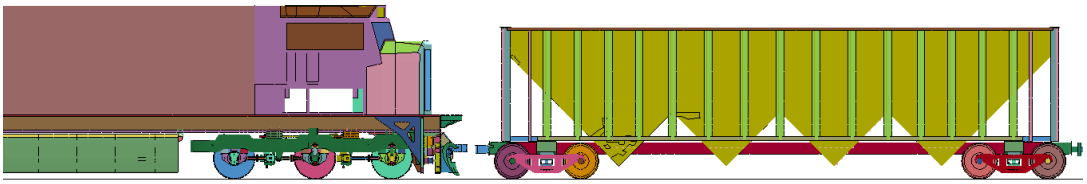

(a) t = 0

(b) t = 300 ms

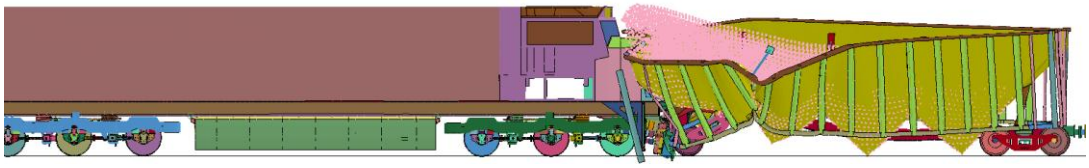

(c) t = 500 ms

Figure 14 Collision simulation of SD70 with CEM: (a) t = 0, (b) t = 300ms; (c) t = 500ms.

The designed maximum energy absorption capacity of the central SEA unit was 9.61×10^6 in-lbf. Simulation results showed the designed crash energy dissipation by the central SEA unit was fully effective (Figure 15(a) and (b)). However, six side SEA units fitted between the modified pilot plate and the reaction plate did not perform as effectively as expected. These distributed SEA units have significantly increased the stiffness of the pilot plates which inhibited the formation of ramps ahead of locomotive front truck. This prevented energy dissipation through locomotive climbing over the hopper car but enabled energy dissipation through extensive structural crushing of the impacted hopper car as displayed in above figures.

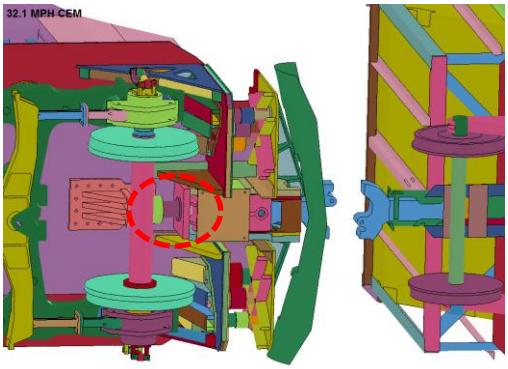

(a) t = 0

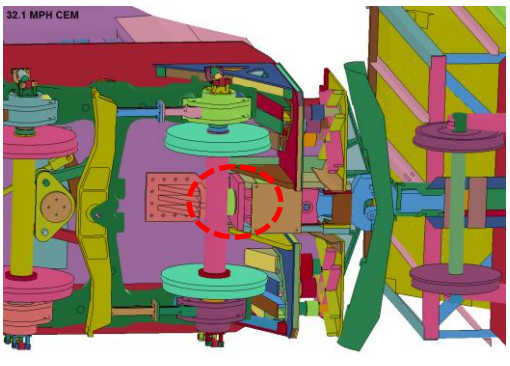

(b) t = 60 ms

Figure 15 Central SEA unit was fully compressed (inside red circles)

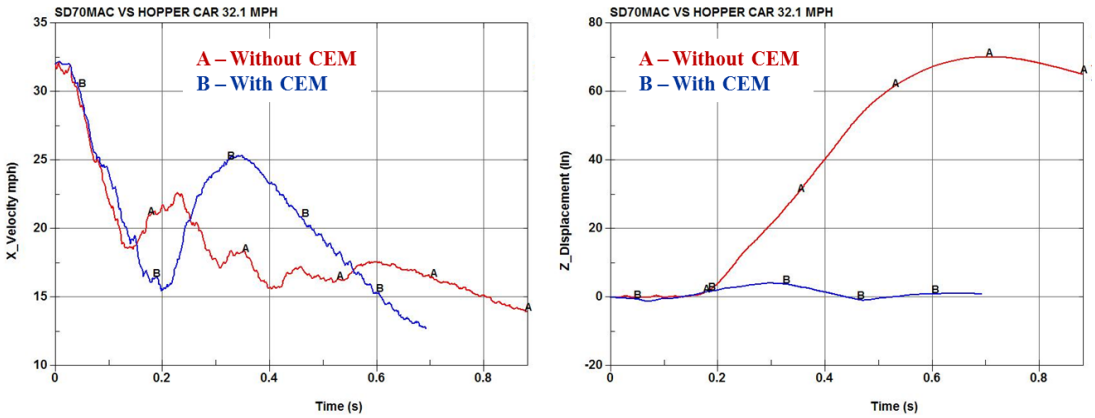

(a) (b)

Figure 16 Time history plots of anti-climber (a): horizontal velocity; (b): vertical displacement.

Detailed examination of the draft gear and the central SEA deformation reveals that the sequence of energy dissipation events such as the shear pin failure, the coupler/draft gear collapse, the sliding of draft gear pocket walls to activate the full plunger displacement of the central SEA unit behind draft gear took place as envisioned in the design of CEM system. Results from the collision simulation of the locomotive with CEM system showed how large amount of crash energy is dissipated in the central SEA unit and extensive deformation of the impacted hopper car and it supports that the intended goal of preventing locomotive override is achieved.

Simulation of Collision between Tank Cars with CEM Installed

In this simulation, the tank car at left side (red) traveled at 15 mph and collided with the middle tank car (blue) which is connected with the tank car at right side (green) through couplers (Figure 17). SEA units with 8.355×10^6 in-lbf energy absorbing capacity were installed at both front and rear ends of each tank car. Each tank car weighed 265,000 lbf. The simulation results showed the crash energy can be fully dissipated by five engaged SEA units and some minor structural deformation of the tank bodies. Cars can be completely stopped within a short time period and derailment was prevented (Figure 18). This shows the potential anti-derailment effects of the CEM system.

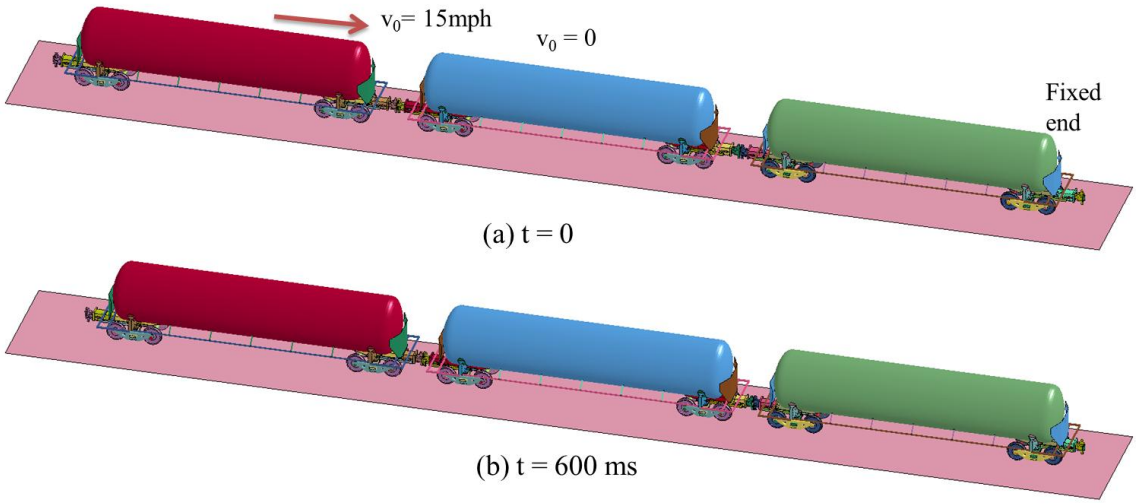

Figure 17 Collision simulation of tank cars with CEM: (a) t = 0; (b) t = 600ms.

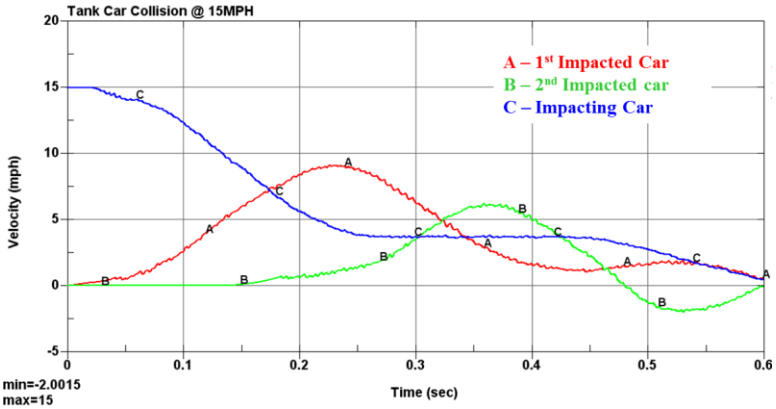

Figure 18 Velocity time history plots of three tank cars.

Conclusions

Through finite element analysis with model validation based on SEA drop test, it shows QNA's recently designed shock energy absorber using UHMW-PE as damping material has great potential in improving railroad safety if the innovative crash energy management systems effectively installed on locomotives, tank cars and other rolling stock. Dynamic finite element simulations discussed in this paper have revealed some advantages of using SPH method in impact analysis involving penetration and large deformation. Further studies are necessary to investigate the rate effect of UHMW-PE in depth and to optimize the capacity and cost of this kind of SEAs. The UHMW-PE based shock energy absorbers can be potentially designed for broad applications in improving crashworthiness in land, marine and aerospace transportation systems.

References

[1] Locomotive Crashworthiness Requirements, Standard S-580, Association of American Railroads, 425 3rd Street, SW., Washington, D.C., 20024, 2004
[2] Manual of Standards and Recommended Practices, Association of American Railroads, 425 3rd Street, SW., Washington, D.C., 20024, 2012
[3] 49 Code of Federal Regulations Part 229 and 238 Locomotive Crashworthiness; Final Rule, Federal Railroad Administration, Department of Transportation, June 27, 2006
[4] APTA Manual of Standards and Recommended Practices for Rail Transit Systems, American Public Transportation Association, 1666 K Street, NW, Washington, DC 20006-1215, USA October, 2004
[5] European Standard EN 15227, Railway applications - Crashworthiness requirements for railway vehicle bodies, European Committee for Standardization, Management Centre: rue de Stassart, 36 B-1050 Brussels, January, 2008
[6] European Standard EN 15551, Railway applications - Railway rolling stocks - Buffers, European Committee for Standardization, Management Centre: Avenue Marnix 17, B-1000 Brussels, November, 2010
[7] LS-DYNA Keyword User's Manual, Volume I and II, Version 971 R6.0.0, Livermore Software Technology Corporation, February, 2012
[8] Ronald Mayville, Richard Stringfellow, Robert Rancatore, and Thomas Hosmer, Locomotive Crashworthiness Research, Volume 1: Model Development and Validation, Final Report, DOT/FRA/ORD-95/08.1, June, 1995
[9] Stephen Kokkins, Wayne Kong and Kash Kasturi, Locomotive Crashworthiness Research: Modeling, Simulation and Validation, Final Report, DOT/FRA/ORD-01/23, July, 2001